

Robustness Analysis of a Position Observer for Surface-Mount Permanent Magnet Synchronous Motors vis-à-vis Rotor Saliency

Harish K. Pillai^{a,*}, Romeo Ortega^b, Michael Hernandez^c, Thomas Devos^c, Francois Malrait^c

^aDept of Elec Engg, IIT Bombay, Mumbai 400076, India

^bLaboratoire des Signaux et Systèmes, CNRS-SUPELEC, 91192 Gif-sur-Yvette, France

^cSchneider Electric, STIE, 33, rue Andre Blanchet, 27120 Pacy-sur-Eure, France

Abstract

A gradient descent-based nonlinear observer for surface-mount permanent magnet synchronous motors (PMSMs) with remarkable stability properties was recently proposed in [7]. A key assumption for the derivation of the observer is the absence of rotor saliency, which is the case in surface-mount PMSMs. A question of great practical interest is to assess the performance of the observer in the presence of saliency. This is the topic of study of the present paper. It is shown that the robustness of the observer is fully determined by the sinusoidal steady-state values of the currents, providing some guidelines for the selection of their reference values to ensure good position estimation.

1. Introduction

Position information is required for field orientation control of PMSMs, which is the industry standard for high-performance applications. In some cases, installing position sensors is troublesome, for instance, in some vacuum pumps, cranes and elevators. Also, in some other applications, like household equipments such as refrigerators and air conditioners, cost constraints stymies the use of speed sensors. The above problems motivate to develop sensorless algorithms for PMSMs, for which numerous works have been published, see [1, 6] for a recent review of the literature.

A very simple observer of the rotor position of PMSMs that exhibits some remarkable stability properties was recently presented in [7]. The analysis, done for the full nonlinear model, proves global (under some conditions, even exponential) convergence of the position estimate and yields very simple robust tuning rules. In [5] the position observer

was combined with an *ad-hoc* linear speed estimator and a standard field-oriented controller, which are often used in applications, yielding very encouraging experimental results. In [8] the position observer is combined with a speed and load torque observer and a passivity-based controller to obtain an asymptotically stable controller that regulates the mechanical speed of the motor, measuring only the electrical coordinates. See also [2, 9] where this observer is also used.

The position observer of [7] is designed for non-salient PMSMs, for which it is possible to derive a gradient descent method—whose robustness properties are well-known. In the phase of saliency, that is present in all practical machines, the gradient cannot be computed and the question of performance of the observer naturally arises. In this paper, we carry out a nonlinear analysis of the effect of saliency on the error equations when the machine is operating in sinusoidal steady-state.

The remaining of the paper is organized as follows. Section 2 presents the model of the salient PMSM. The observer of [7] is briefly recalled in Section 3 and the error equations due to the presence of saliency are derived in Section 4. Some observations about the equilibria of these equations are listed in Section 5 alongwith some representative simulation diagrams.

*Corresponding author

Email addresses: hp@ee.iitb.ac.in (Harish K. Pillai), ortega@lss.supelec.fr (Romeo Ortega), michael.hernandez@fr.schneider-electric.com (Michael Hernandez), thomas.devos@fr.schneider-electric.com (Thomas Devos), francois.malrait@fr.schneider-electric.com (Francois Malrait)

Preprint submitted to Elsevier

May 30, 2013

2. Mathematical Model of Salient PMSM

The classical fixed-frame $\alpha\beta$ -model of the PMSM in sinusoidal regime establishes the relation between the voltages and currents as [3, 4]

$$v_{\alpha\beta} = Ri_{\alpha\beta} + \frac{d}{dt}\lambda_{\alpha\beta} \quad (1)$$

where $\lambda_{\alpha\beta} = (\lambda_\alpha, \lambda_\beta) \in \mathbb{R}(i_d^0)^2$, $i_{\alpha\beta} = (i_\alpha, i_\beta) \in \mathbb{R}(i_d^0)^2$ and $v_{\alpha\beta} = (v_\alpha, v_\beta) \in \mathbb{R}(i_d^0)^2$ are the flux linkages, the currents and the voltages in the α and β phases, respectively, and R is the resistance of the stator coils. In the unsaturated case the flux linkages are defined by

$$\begin{aligned} \lambda_\alpha &= L_{\alpha\alpha}i_\alpha + L_{\alpha\beta}i_\beta + \lambda_m \cos n\theta \\ \lambda_\beta &= L_{\beta\alpha}i_\alpha + L_{\beta\beta}i_\beta + \lambda_m \sin n\theta \end{aligned} \quad (2)$$

where $L_{\alpha\alpha}$ and $L_{\beta\beta}$ are self inductances of α and β phases, respectively, and $L_{\alpha\beta}$ and $L_{\beta\alpha}$ are the mutual inductances between the two phases.¹ λ_m is the magnetic flux due to the permanent magnet in the rotor, $n\theta$ is the electrical angle between the α -phase and the rotor axis—where θ is the mechanical angle between the α -phase and the rotor axis and n is the number of pole-pairs in the machine.

For the salient machine, the self and mutual inductances of the phases vary with the electrical angle between the phases and the rotor axis. A model that captures this variation is given by the following equations

$$\begin{aligned} L_{\alpha\alpha} &= L_s + L_g \cos 2n\theta \\ L_{\beta\beta} &= L_s - L_g \cos 2n\theta \\ L_{\alpha\beta} &= L_{\beta\alpha} = L_g \sin 2n\theta, \end{aligned}$$

Substituting these equations into (2) gives the equation

$$\lambda_{\alpha\beta} = [L_s + L_g Q(\theta)]i_{\alpha\beta} + \lambda_m c(\theta), \quad (3)$$

where, to simplify the notation, we have defined

$$Q(\theta) := \begin{bmatrix} \cos 2n\theta & \sin 2n\theta \\ \sin 2n\theta & -\cos 2n\theta \end{bmatrix}, \quad c(\theta) := \begin{bmatrix} \cos n\theta \\ \sin n\theta \end{bmatrix}. \quad (4)$$

The final model of the salient PMSM is then given by (1), (3) and (4). A non-salient machine is modeled with the same equations, under the assumption that $L_g = 0$.

¹As is standard practice, and without loss of generality, we assume $L_{\alpha\beta} = L_{\beta\alpha}$.

The observer problem is to generate a convergent estimate of θ from the measurements of $i_{\alpha\beta}$ and $v_{\alpha\beta}$, and the knowledge of the (positive constant) physical parameters R, L_s, L_g and λ_m .

3. The Position Estimator of [7]

From (3) it is obvious that if the flux is known, and $L_g = 0$, it is possible to reconstruct θ via the trigonometric identity

$$\theta = \tan^{-1} \left(\frac{\lambda_\beta - L_s i_\beta}{\lambda_\alpha - L_s i_\alpha} \right).$$

On the other hand, from (1) it is clear that one can estimate the flux $\lambda_{\alpha\beta}$ (up to a constant due to the unknown initial conditions) by integrating a quantity that depends on the measured quantities. The key observation of [7] is that a gradient can be computed to add to this integral a correction term that will drive the estimation in the right direction. More precisely, consider the following equations

$$\begin{aligned} \dot{x} &= v_{\alpha\beta} - Ri_{\alpha\beta} \\ y &= |x - L_s i_{\alpha\beta}|^2, \end{aligned}$$

with $|\cdot|$ the standard Euclidean norm. Clearly, x estimates the flux $\lambda_{\alpha\beta}$ up to a constant. Now, note that in the case of no saliency, equation (3) loses the middle term involving L_g and therefore $y = \lambda_m^2$ when $x = \lambda_{\alpha\beta}$. Therefore, it is reasonable to propose a gradient search that tries to minimize the criterion $(\lambda_m^2 - |x - L_s i_{\alpha\beta}|^2)^2$, which leads to the flux observer proposed in [7]

$$\dot{x} = v_{\alpha\beta} - Ri_{\alpha\beta} + \gamma(x - L_s i_{\alpha\beta})(\lambda_m^2 - |x - L_s i_{\alpha\beta}|^2) \quad (5)$$

where $\gamma > 0$ is a scaling factor.

For the salient machine $L_g \neq 0$, bringing into (3) an unknown θ -dependent term. It is not clear how to formulate a criterion with a computable gradient in this case. In this paper, we analyze the performance of the flux observer designed for the non-salient machine [7], when applied to a machine with saliency.

4. Error Equations

In this section, the dynamics of the observation errors are derived and presented in a suitable rotating frame for the analysis of their equilibria. To

streamline the presentation we introduce the rotation matrix

$$\exp(-n\theta J) = \begin{bmatrix} \cos n\theta & \sin n\theta \\ -\sin n\theta & \cos n\theta \end{bmatrix},$$

where

$$J := \begin{bmatrix} 0 & -1 \\ 1 & 0 \end{bmatrix}.$$

Notice that this matrix defines the well-known transformation from $\alpha\beta$ to dq coordinates [4]. In particular, the i_d and i_q currents are given by

$$i_{dq} = \exp(-n\theta J)i_{\alpha\beta}.$$

As will become clear below the values of these currents will play a fundamental role on the performance of the observer.

Proposition 4.1. *Consider the salient PMSM model (1), (3) and (4) together with the flux observer (5). Define the error signals $e = x - \lambda_{\alpha\beta}$ and its scaled and rotated form*

$$\xi = -\frac{1}{\lambda_m} \exp(-n\theta J)e. \quad (6)$$

Introduce, moreover, the time-scale change

$$\frac{dt}{d\tau} = \frac{1}{\gamma\lambda_m^2}.$$

Then,

$$\begin{aligned} \frac{d\xi_1}{d\tau} &= \Omega\xi_2 - \sigma(\xi)(\xi_1 - i_d^0 - 1) \\ \frac{d\xi_2}{d\tau} &= -\Omega\xi_1 - \sigma(\xi)(\xi_2 + i_q^0) \end{aligned} \quad (7)$$

where

$$\sigma(\xi) := (\xi_1 - i_d^0 - 1)^2 + (\xi_2 + i_q^0)^2 - 1, \quad (8)$$

with the scaled currents i_{dq}

$$i_{dq}^0 := \begin{bmatrix} i_d^0 \\ i_q^0 \end{bmatrix} := \frac{L_g}{\lambda_m} i_{dq}$$

and the scaled speed

$$\Omega = \frac{n}{\gamma\lambda_m^2} \dot{\theta}.$$

Proof. From (3)²

$$\begin{aligned} x - L_s i_{\alpha\beta} &= e + \lambda_{\alpha\beta} - L_s i_{\alpha\beta} \\ &= e + L_g Q i_{\alpha\beta} + \lambda_m c. \end{aligned}$$

²In the sequel the arguments of the functions are omitted.

Thus,

$$\begin{aligned} |x - L_s i_{\alpha\beta}|^2 &= |e + L_g Q i_{\alpha\beta} + \lambda_m c|^2 \\ &= |e|^2 + L_g^2 |i_{\alpha\beta}|^2 + \lambda_m^2 \\ &\quad + 2L_g e^\top Q i_{\alpha\beta} + 2\lambda_m e^\top c \\ &\quad + 2\lambda_m L_g c^\top Q i_{\alpha\beta} \end{aligned}$$

and

$$\begin{aligned} \lambda_m^2 - |x - L_s i_{\alpha\beta}|^2 &= -|e|^2 - L_g^2 |i_{\alpha\beta}|^2 \\ &\quad - 2L_g e^\top Q i_{\alpha\beta} - 2\lambda_m e^\top c \\ &\quad - 2\lambda_m L_g c^\top Q i_{\alpha\beta}. \end{aligned}$$

Thus, the error dynamics is

$$\begin{aligned} \dot{e} &= \dot{x} - \dot{\lambda} \\ &= \gamma[-|e|^2 - L_g^2 |i_{\alpha\beta}|^2 - 2L_g e^\top Q i_{\alpha\beta} \\ &\quad - 2\lambda_m e^\top c - 2\lambda_m L_g c^\top Q i_{\alpha\beta}] \times \\ &\quad (e + L_g Q i_{\alpha\beta} + \lambda_m c) \end{aligned} \quad (9)$$

Now, differentiating (6) we get

$$\dot{\xi} = -n \frac{d\theta}{dt} J \xi - \frac{1}{\lambda_m} \exp(-n\theta J) \dot{e}$$

On simplifying, we get

$$\dot{\xi} = -n\dot{\theta} J \xi - \gamma\lambda_m^2 \sigma(\xi) \begin{bmatrix} \xi_1 - i_d^0 - 1 \\ \xi_2 + i_q^0 \end{bmatrix}.$$

The proof is completed introducing the time scaling. $\square\square\square$

Remark 1. The equations (7) fully describe the behavior of the position observer (5) when applied to a salient machine. Note that the functions i_d^0 and i_q^0 play a central role in the error equations (7)—in the steady-state operation of the machine they are constants, proportional to the currents i_d and i_q . Note that the scaling factor $\frac{L_g}{\lambda_m}$ is, in some sense, a measure of the saliency of the machine as it depends on L_g scaled by the magnetic flux of the permanent magnet of the machine.

5. Observations about the Error Equations

For the sake of brevity, we now list several observations about existence and location of equilibria for the error equations (7), when i_{dq} is constant—that is, for the machine operating in steady-state. We have also added relevant figures from simulations that support these observations. Formal proofs of these observations would be reported elsewhere.

- For a nonzero Ω , every equilibrium point of the error equations lie on a critical circle defined by

$$C(\xi) := \frac{\left(\xi_1 - \frac{i_d^0 + 1}{2}\right)^2 + \left(\xi_2 + \frac{i_q^0}{2}\right)^2}{\frac{(i_d^0 + 1)^2 + (i_q^0)^2}{4}}$$

- For fixed values of Ω , i_d^0 and i_q^0 , there is at least one equilibrium point and at most three equilibrium points.
- When more than one equilibrium point exists, then $\Omega \leq \frac{1}{3}$ and $(1 + i_d^0)^2 + (i_q^0)^2 \geq \frac{8}{9}$.
- The origin is an equilibrium point if and only if $\sigma(\xi) = 0$ or $\sigma(\xi) = -1$. Note that the case of a non-salient machine falls in this category as $L_g = 0$ and therefore $\sigma(\xi) = 0$.
- The disk

$$\{\xi \in \mathbb{R}^2 \mid |\xi| \leq 1 + \sqrt{(i_d^0 + 1)^2 + (i_q^0)^2}\}$$

is globally asymptotically stable (GAS).

- If $(i_d^0 + 1)^2 + (i_q^0)^2 = 1$, then
 - a) If $0 < \Omega < 1/2$, then there are three equilibria. The origin is a stable node, whereas the other two equilibrium points are a saddle and an unstable equilibrium point.
 - b) If $\Omega = 1/2$, then there are two equilibria.
 - c) If $\Omega > 1/2$, then the origin is the only equilibrium. It is a stable node for $\Omega \leq 1$ and a stable focus for $\Omega > 1$.
- If $(i_d^0 + 1)^2 + (i_q^0)^2 > 1$, then there exists an equilibrium point ξ^* , such that $\sigma^* = \sigma(\xi^*) > 0$. This equilibrium point is stable. If $(\sigma^* + 1) \geq \Omega$, then ξ^* is a stable node, otherwise it is a stable focus.
- If $(i_d^0 + 1)^2 + (i_q^0)^2 \leq 1/2$, then there exists only one equilibrium point, which is unstable. However, a stable limit cycle also exists in this case, whose basin of attraction is the whole plane minus the equilibrium point.
- If $1/2 < (i_d^0 + 1)^2 + (i_q^0)^2 < 8/9$, then there exists only one equilibrium point. For low speeds, the equilibrium point is unstable and there exists a limit cycle. At higher speeds, the equilibrium point becomes a stable focus.

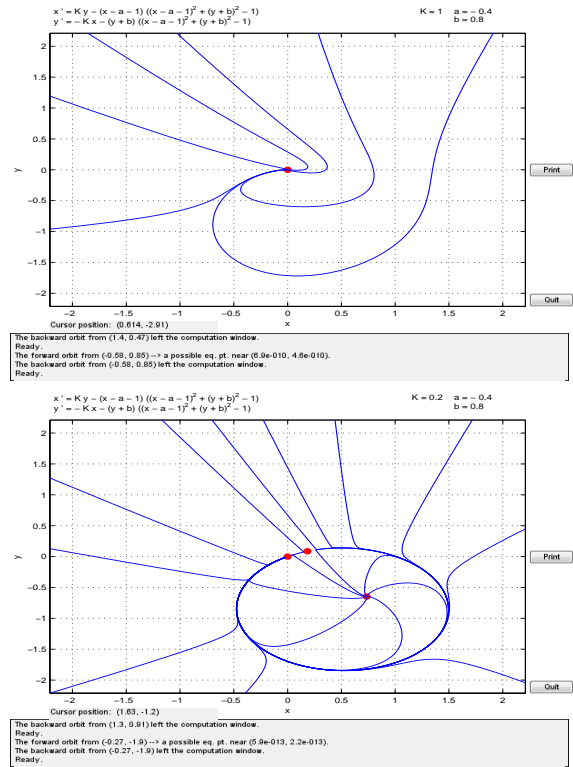


Figure 1: The case of $(i_d^0 + 1)^2 + (i_q^0)^2 = 1$ having one and three equilibrium points

- If $1 > (i_d^0 + 1)^2 + (i_q^0)^2 \geq 8/9$, then there exists two critical speeds $\Omega_1 < \Omega_2$, such that
 - a) if $\Omega < \Omega_1$, then only one equilibrium point exists. For low speeds, this equilibrium point is unstable and there exists a limit cycle around this equilibrium point. As the speed increases, the limit cycle shrinks until finally it opens out and the equilibrium point becomes a stable focus.
 - b) if $\Omega_1 \leq \Omega \leq \Omega_2$, then there are three equilibrium points. One of them is stable, a second one is a saddle and a third one is an unstable equilibrium point.
 - c) if $\Omega > \Omega_2$, then there exists only one equilibrium point, which is stable.

The case of $(i_d^0 + 1)^2 + (i_q^0)^2 = 1$ and having one stable equilibrium point is displayed in Figure 1a. Notice that the origin is a stable focus in this case. The situation of three equilibrium points appearing

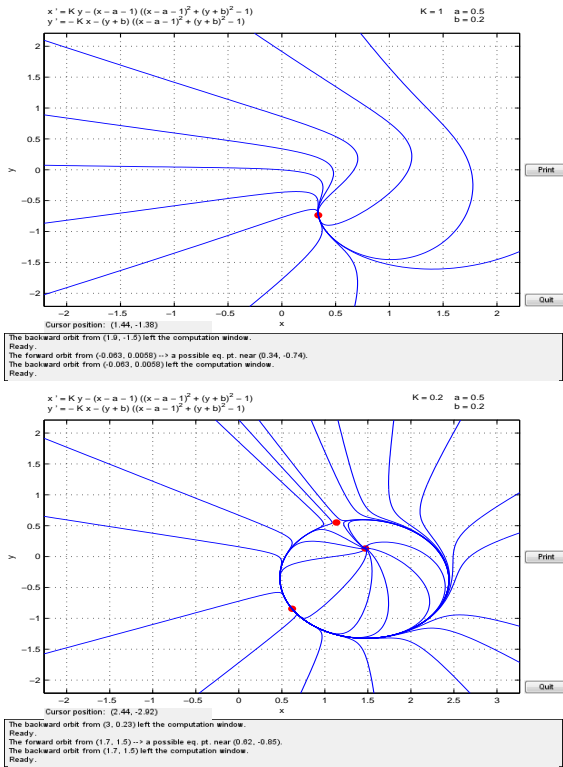


Figure 2: Various cases of equilibrium points when $(i_d^0 + 1)^2 + (i_q^0)^2 > 1$

for the case $(i_d^0 + 1)^2 + (i_q^0)^2 = 1$ is displayed in Figure 1b. Again notice here that the origin is a stable equilibrium point (in fact, a stable node). Among the other two equilibrium points, the one nearer to the origin is a saddle, whereas the one further away is an unstable focus.

The case of $(i_d^0 + 1)^2 + (i_q^0)^2 > 1$ and having one stable equilibrium point is displayed in Figure 2a, whereas a case of three equilibrium points is displayed in Figure 2b. Of the three equilibrium points, the one closest to the origin is a stable equilibrium point (in fact, a stable node). Among the other two equilibrium points, the one appearing towards the top of the diagram is a saddle, whereas the one further to the right is an unstable focus.

In Figure 3, we have a case where $(i_d^0 + 1)^2 + (i_q^0)^2 \leq 1/2$. The equilibrium point is an unstable focus. Observe that there exists a limit cycle around the equilibrium point. This limit cycle is stable, as in all points other than the equilibrium point, eventually evolves towards this limit cycle.

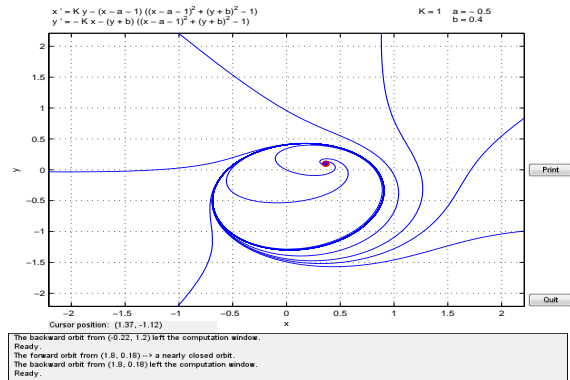


Figure 3: The case of $(i_d^0 + 1)^2 + (i_q^0)^2 < 1/2$ having an unstable equilibrium point and a limit cycle

Figure 4 shows the various cases arising when $8/9 \leq (i_d^0 + 1)^2 + (i_q^0)^2 < 1$. Thus Figure 4a is a case of $\Omega > \Omega_2$: one stable equilibrium point. Figure 4b is the case of $\Omega_1 < \Omega < \Omega_2$: three equilibrium points with one stable, one unstable focus and the third a saddle. Figure 4c is the case of $\Omega < \Omega_1$: one unstable equilibrium point with a limit cycle around it.

6. Conclusions

We have done a theoretical analysis of the sensorless position observer given in [7] for non-salient machines. Only under the condition of $(i_d^0 + 1)^2 + (i_q^0)^2 = 1$, would the origin be an equilibrium point of the error dynamics. Thus, it is only under this very specific condition that the error in estimation of flux can actually go to zero. In all the other cases, there is some error in the estimated flux and therefore the estimated position. However, this error is never very large—a globally attractive disc exists for the error system.

Under specific conditions, three equilibrium points can exist. When three equilibrium points do exist, the one closest to the origin is a stable equilibrium. The other two equilibrium points are a saddle and an unstable node/focus. In all other cases, there is only one equilibrium point which is either a stable equilibrium point or an unstable equilibrium with a stable limit cycle around the unstable equilibrium point.

References

- [1] P. P. Acarnley and J. F. Watson, Review of position-sensorless operation of brushless permanent-magnet machines, *IEEE Trans. on Ind. Electron.*, vol. 53, no. 2, pp.352-362, Apr. 2006.
- [2] W. Dib, R. Ortega and J. Malaize, Sensorless control of permanent-magnet synchronous motor in automotive applications: Estimation of the angular position, *IECON'11*, November 7–10, 2011, Melbourne, Australia.
- [3] S. Ichikawa, M. Tomita, S. Doki and S. Okuma, Sensorless control of PMSM using on-line parameter identification based on system's identification theory, *IEEE Trans Industrial Electronics*, Vol. 53, No. 2, pp. 363–373, April 2006.
- [4] P.C. Krause, **Analysis of Electric Machinery**, McGraw Hill, New York, 1986.
- [5] J. Lee, K. Nam, R. Ortega, L. Praly and A. Astolfi, Sensorless control incorporating a nonlinear observer for surface-mount permanent magnet synchronous motors, *IEEE Transactions on Power Electronics*, Vol. 25, No. 2, pp. 290–297, 2010.
- [6] K. Nam, **AC Motor Control and Electric Vehicle Applications**, CRC Press, 2010.
- [7] Ortega R., L. Praly, A. Astolfi, J. Lee and K. Nam, Estimation of rotor position and speed of permanent magnet synchronous motors with guaranteed stability, *IEEE Transaction on Control Systems Technology*, vol 19, no 3, pp 601 – 614, May 2011.
- [8] D. Shah, G. Espinosa, R. Ortega and M. Hilaret, “An asymptotically stable sensorless speed controller for non-salient permanent magnet synchronous motors”, *18th IFAC World Congress*, Aug. 28–Sept. 2, 2011, Milano, Italy. (To appear in *Int. J. on Robust and Non-linear Control*.)
- [9] P. Tomei and C. Verrelli, Observer-based speed tracking control for sensorless PMSM with unknown torque, *IEEE Trans. Automat. Contr.*, Vol. 56, No. 6, June 2011, pp. 1484–1488.

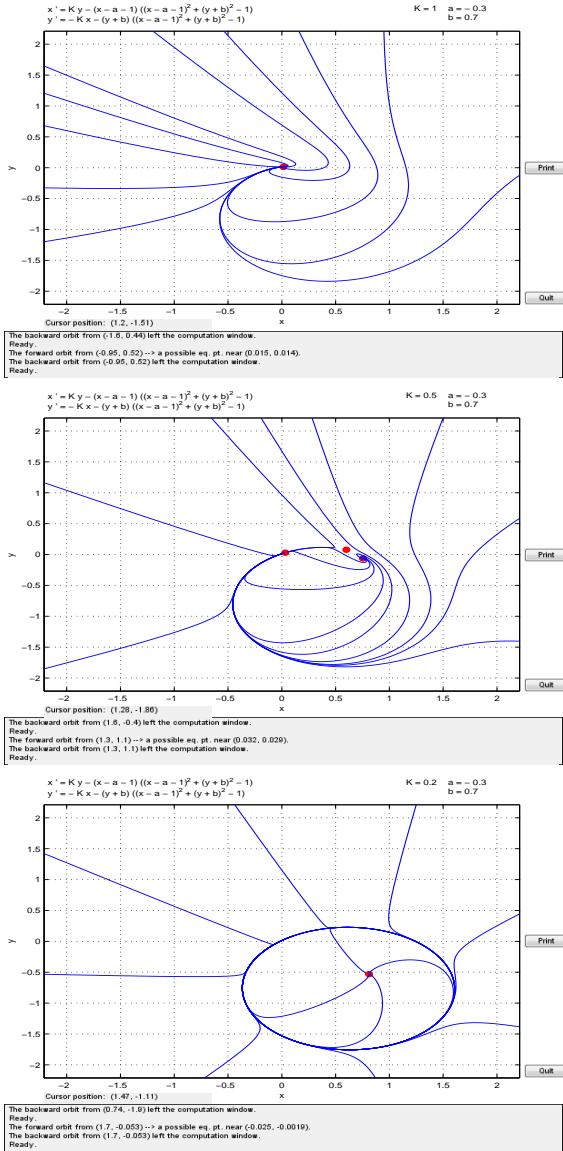


Figure 4: Different cases arising when $8/9 \leq (i_d^0 + 1)^2 + (i_q^0)^2 < 1$